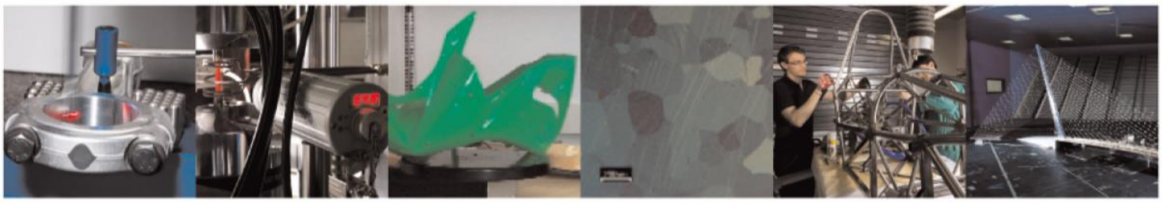

Mechanical and wear performance of A356/Al2O3 aluminum nanocomposites by considering the mechanical milling time and microstructural properties

Caliskan, O.; Sunar, T.; Ozyurek, D.

Mechanical and wear performance of $A356/Al_2O_3$ aluminium nanocomposites by considering the mechanical milling time and microstructural properties.

Abstract

Purpose of this paper

The paper examines the mechanical and wear performance of $A356/Al_2O_3$ (alumina) nanocomposites. The correlation between wear performance and the microstructural properties that result from various mechanical milling periods was investigated.

Design/methodology/approach

The production of nano alumina reinforced (1 wt.%) A356 aluminium nanocomposite specimens were carried out using the traditional powder metallurgy method, incorporating three different mechanical milling times (1, 2, and 4 hours). Subsequently, mechanical and wear performance assessments were conducted using hardness, compression, and pin-on-disc wear tests.

Findings

Although the specimens subjected to the most prolonged mechanical milling (4 hours) demonstrated superior hardness and compressive strength properties, they exhibited a remarkable weight loss during the wear tests. The traditional evaluation, which supports that the wear performance is generally correlated with hardness, does not consider the microstructural properties. Since the sample milled for one hour has a moderate microstructure, it showed better wear performance than the sample with higher hardness.

What is original/value of paper

The originality of the paper is demonstrated through its evaluation of wear performance, incorporating not only hardness but also the consideration of microstructural properties resulted from mechanical milling.

Keywords: Aluminium matrix composites, Nanoparticles, Wear testing

1. Introduction

Metal-matrix nanocomposites – have at least one nanosized component – can provide different functional properties. While mechanical strength increases, their ductility remains at an acceptable level (Mazahery and Shabani, 2012). Nanocomposites can be produced by liquid-state (stir and squeeze casting, infiltration, etc.) and solid-state (powder metallurgy). There are also derivative applications such as hot pressing, compocasting and friction stir process (Celebi et al., 2018; Bobic et al., 2018; Akbari and Asadi, 2021; Akbari and Asadi, 2022). Powder Metallurgy (PM), a solid-state production method, provides low processing temperatures. The homogeneous distribution of the reinforcements can be achieved more easily by the controllable nature of PM. Mechanical milling (MM), a high-energy ball grinding method, is an alternative mixing method for powder preparation phase. In this method, the powders are bonded through mechanical deformation. Thus, the reinforcement particles are dispersed more homogeneously in the matrix (Özyürek and Tekeli, 2010). Common reinforcement particles are the hard ceramic materials such as SiC, B_4C, TiB_2, and Al_2O_3 (Özyürek et al., 2012; Erek and Özyürek, 2017; Özyürek and Çiftçi, 2011; Şimşek et al., 2020; Akbari et al., 2018; Akbari et al., 2022), and often used as reinforcement materials in micro/nanocomposites. Besides, there are studies on nano-reinforced composites at low reinforcement rates in the literature (Shivakumar et al., 2015; Vencl et al., 2022; Sunar and Özyürek, 2022). The addition of hard reinforcement particles positively affects the mechanical properties. Studies also examine the effects of MM time on the final powder size and the mechanical properties of the produced material (Akhlaghi et al., 2019; Safari et al., 2013). The reduction in the reinforcement particle size by MM, increases the hardness and strength of the composites and minimizes the loss in ductility (Rahimian et al., 2010). Although there are various studies – zinc-aluminum/B_4C and graphite, Al6061/carbon nanotube, A6061/Al_2O_3 nanocomposites (Güler et al., 2020; Omidi et al., 2017; Hoseini et al., 2010) – on the wear performance of nanocomposites produced with different aluminum alloys and reinforcement particles, similar research has yet to be found on the A356 alloy.

A novel aspect of this investigation is the evaluation of mechanical behavior, and wear resistance of A356/Al_2O_3 nanocomposites by considering the microstructural outcomes by MM. A356 and nano Al_2O_3 powders were subjected to MM using varying durations. Subsequently, the microstructural characteristics, hardness, compression strength, and pin-on-disc wear behavior of the resulting nanocomposite samples were analyzed.

2. Materials and Methods

A356 aluminium alloy powders (LPW Technology Ltd., particle size range: 20-63 µm) were used as a matrix and nano Al_2O_3 powders (Nanografi Ltd., average particle size: 20 nm) were used as reinforcements with a constant ratio of 1 wt.%. The mixture was milled using Fritsch planetary ball milling device (capacity: 225 ml) with following parameters: 400 rpm; 1/2/4 hours; 1/10 ball/powder ratio (stainless steel balls with 8 mm diameter) and 1% of stearic acid was added as process control agent. The operation was paused for 15 minutes for every 15 minutes to prevent the powders from overheating. Malvern Mastersizer 3000 Particle Size Analyzer was used for particle size measurements. Powders were cold pressed uniaxially with 520 MPa in a cylindrical form of a diameter of 12 mm and a height of 8 mm. Sintering is applied at 550 °C for 1 hour, in a vacuum environment (10^{-6} mbar, constant heating and cooling rate 4°C min^{-1}). The density of sintered samples was measured according to Archimedes' principle using a PRECISA XB200h density measurement kit. Hardness measurements were carried out using a Shimadzu micro-hardness tester (HV0.5: 500gf load applied for 15 seconds) on the top surface, and cross-sections of the samples. The compression test samples were fabricated by machining them to a diameter and height of 8 mm. Compression tests were carried out according to ASTM E9 standards at a constant crosshead speed (0.001 sec^{-1}) using a Zwick/Roell Z600 tester with a load capacity of 600 kN. The standard pin-on disc assembly was used for wear tests. AISI 4140 steel with an average hardness of 64 HRC was used as the counter disc. Wear tests were carried out under dry conditions and at room temperature in accordance with ASTM G99 standards. 1ms^{-1} sliding speed, 30N load, and 4 different sliding distances (500, 1000, 1500, and 2000 m) were used in wear tests. The hardness and wear performance investigations were applied after sintering. The samples were weighed on a precision scale (precision: 10^{-4}g) to determine weight losses. Wear rates were calculated using the following equation.

$$W_a = \Delta G/d\,.P.S \qquad \text{Eq. (1)}$$

In the equation (1), W_a is the wear rate ($mm^3\ N^{-1}m^{-1}$); ΔG is the weight loss (g); P is the load (N); S is the sliding distance (m) and d is the density ($g\ cm^{-3}$).

3. Results and Discussions

3.1. Powder size and Density

The average powder size of the MM'ed powders was measured after each MM operation and the cumulative powder size frequencies are given in Figure 1.a. The powder size shows an upward trend in the initial stages of MM. Notably, between 1 and 2 hours, the powder size increases from 55.6 µm to 95.7 µm. The increase in powder size is the result of bonding caused by impacts between the ball-powder-ball and ball-powder-chamber wall during ball milling (Akhlaghi et al., 2019). The average powder size decreased to 66.5 µm after 4 hours of milling, with a tendency to decrease after 2 hours. This phenomenon can be attributed to the sequential deformation mechanism of MM). During ball milling, clean surfaces are consistently produced on powders (Suryanarayana, 2001). As milling progresses, the powders that undergo continuous deformation become harder and are prone to fracture due to excessive plastic deformation. The powder size increases because of cold welding and decreases due to fracturing (Safari et al., 2013).

Deformation during the MM process leads to complex-shaped particles with increased surface area, resulting in higher porosity. As shown in Figure 1.b, the micropores formed during compression grow during sintering, leading to an increase in relative density (Yildirim et al., 2020). The density of the nanocomposites decreases almost linearly with an increase in MM time, while particle size increases interruptedly with a decrease at higher MM time, as seen in Figure 1.a. Powders subjected to excessive plastic deformation during high-energy milling undergo deformation hardening, which makes shaping them challenging during cold pressing (Safari et al., 2013). The compressibility of composite powders decreased with an increase in MM time in a previous study (Rahimian et al., 2010), restricting the packaging of green compacts and increasing the amount of pore while decreasing the density.

Figure 1. Mechanical and physical properties of the samples, a) cumulative size frequency-particle diameter data, b) density and hardness results.

3.2.Microstructure

Figure 2 displays optical microscope images taken from the cross-sections of nanocomposite samples, revealing the effect of MM on grain size. Samples MM'ed for 1h and 2h have more spherical grains, likely due to less exposure to MM, resulting in lower hardness and a return to a more natural form during sintering. In contrast, samples MM'ed for 2h display larger grains in microstructure images due to cold welding and bonding of particles, leading to sequential deformation and grain growth. Nanocomposites MM'ed for 4 hours have smaller particle size, resulting in decreased grain size. The extreme plastic deformation of particles during 4h of MM is clearly visible from the shape of the grains.

Figure 2. Optical images of microstructure of A356/ nano Al_2O_3 samples MM’ed for 1 hour (a), 2 hours (b) and 4 hours (c).

Figure 3 shows the SEM images of the microstructures of A356 alloy and nanocomposites. When the SEM images are examined, it is understood that the matrix is Al (dark grey zones), while the light grey phase appears to be homogeneously distributed within the microstructure is Si according to the EDS results (Figure 3.a). Particle boundaries appear on the sample surfaces as thin black lines, while the pores formed in the structure are in the form of large black zones (pore). The similar appearance of microstructures of powder particles is understandable because there was a constant 1 wt. % nano-Al_2O_3.

Figure 3. SEM images of the microstructure of samples; a) A356 alloy, b) A356/nano Al_2O_3 nanocomposites MM’ed for 1h, c) A356/nano Al_2O_3 samples MM’ed for 2h, d) A356/nano Al_2O_3 samples MM’ed for 4h.

3.3.The hardness and compressive test results

A356 alloys are known to have relatively low hardness values after fabrication (or non-milled in this case)(Vencl et al., 2020).The hardness results measured from the top surfaces of the samples were given in Figure 1.b The hardness increased with the increase in MM time. While the average hardness values of the samples MM'ed for 1 hour were 70.71 HV, this hardness value was measured as 72.57 HV for the samples MM'ed for 2 hours. Negligible increase was measured in hardness between 1 and 2 hours of MM. It can be said that this fluctuation is due to the hardening of the powders with the difference in the MM time of 1 hour. On the other hand, average hardness value increased significantly to 95.7 HV for nanocomposites MM'ed for 4 hours. This increase is thought to be due to work hardening and the reduction in powder sizes. Increasing the hardness of the powders makes re-deformation more difficult. In addition, the compressibility of powders decreases with increasing MM time (Fogagnolo et al., 2010). Hardness measurements from cross-sections were also showed similar results with hardness of top surfaces. Figure 4 shows the hardness values of the from cross-sections of nanocomposite samples. The hardness of the top and bottom regions was observed to be higher than the middle regions for the sample MM'ed for 4h. The samples MM'ed 1h and 2h did not show this type of hardness gradient. Moreover, lower hardness values were measured from top and bottom surfaces for that samples.

Figure 4. Hardness measurements from cross-sections of A356/nano Al_2O_3 samples MM'ed for 1, 2 and 4 hours.

Figure 5 gives the compression test results displaying the stress-strain curves of nanocomposite samples (Figure 5.a), and the mean values of yield stresses (Figure 5.b). The results clearly illustrate that higher reinforcement ratios provide higher compression strength as well as hardness. Nanocomposites MM'ed for 1h and 2h showed similar compression strength while the 2h of MM showed slightly higher yield stress. On the other hand, nanocomposites MM'ed for 4h showed relatively better compressive strength results. The Al_2O_3 nanoparticles improved the strength of the composites, even if they have lower relative densities (4h MM'ed). The samples consist of smaller and harder particles provide better compressive properties. The increase in hardness and compressive strength can be explained in two ways. The first is that deformation hardening occurs in composite powders with the effect of high-energy ball milling. In other words, nanocomposite powders undergo more deformation with the increase in milling time leads to an increase in hardness and compressive strength. The second, which is valid for nanocomposites MM'ed for 4h is that the decrease in particle size due to MM strengthen the nanocomposites by well-known grain-boundary strengthening (Hall-Petch) mechanism (Safari et al., 2013; Tiku et al., 2020). However, considering the particle size results given in Figure 1.a, it is observed that the hardness of nanocomposites MM'ed for 2-hour increased as close as the nanocomposites which has smaller particles (nanocomposites MM'ed for 1-hour). The reason for the increase in hardness was related to deformation hardening in composite powders due to MM time. Powders undergo further deformation when subjected to MM for longer periods of time, that causes work hardening even though the particle size increases with cold welding. In addition, hardness is known to increase due to nanoparticles in the matrix restricting or preventing the dislocation movement (Orowan mechanism).

Figure 5. Compression test results of nanocomposite samples; a) Stress-strain data, b) Yield stress values.

3.4.Wear test results

Figure 6 shows the weight loss (a), wear rate (b) and average friction coefficient results (c) for different sliding distances. The weight loss results given in Figure 6.a indicate that the highest weight loss was measured from the samples MM'ed for 4 hours, while the lowest weight loss was observed at the samples which MM'ed for 1 hour. The wear rate results increased by particle reinforcement and mechanical alloying agree with the results of similar materials in the literature but are slightly lower. (Gibson et al., 1984; Vencl et al., 2019; Yang et al., 2004). The reasons for the relatively lower wear rate may be the different types of reinforcement particles used, their size –nano– and the use of MM'ed powders. There is a general interpretation that the hardness is primarily effective parameter to the wear rate (Hosseini et al., 2012; Edalati et al., 2014; Moazami-goudarzi and Akhlaghi, 2016). Most of the studies conducted on the wear properties of metal matrix composites consist of Archard equation (Archard, 1953). Archard equation indicates that volume of worn material is affected by the normal force, the sliding distance, wear coefficient and the hardness of the material. According to this theory, nanocomposite samples MM'ed for 4 hours are expected to show the lowest weight loss due to their higher hardness and strength, however, the highest weight loss values occurred in these samples (See section 3.3). As a result of wear tests, it was also revealed that there was an inconsistency between the weight loss results and the hardness results. Here, there is one point that needs to be emphasized. The wear coefficient can take many different values (at least up to seven orders of magnitude), which limits the predictive power of this law (Popov, 2019). Wear coefficients of the samples were targeted to be equal or similar because there was constant reinforcement ratio (1% wt. Al_2O_3) for each sample. In fact, different friction coefficient values were resulted from the tests given in Figure 6.c. The friction coefficient raw sample data for MM'ed for 2h were illustrated as an example. Therefore, different wear mechanisms override when the MM time of nanocomposite powders changes due to microstructure modification. When the weight loss results are evaluated together with the relative density and microstructure results, it is seen that there is a parallelism between the pore amount and weight loss. The improved weight loss and wear rate results observed in the nanocomposite mixed for 1 hour (MM'ed 1h) are attributed to its moderate grain size and increased density. A smoother wear mechanism is observed when there is reduced porosity and a moderate microstructure featuring finer and more uniformly distributed grains. This is due to the higher ductile structure that prevents sudden exposure to extreme forces. Higher porosity causes more fractures during wear tests, leading to increased weight loss. Pores formed in the structure make it easier to deform during wear tests, triggering wear mechanisms such as delamination or fracture in later stages, thereby reducing the wear performance of the composite with higher weight loss.

The wear resistance of the nanocomposite materials decreased with increasing mechanical milling time due to increased porosity and a decrease in hardness – for ZA27/B_4C/graphite (Güler et al., 2020) –, and the formation of microcracks, which acted as a channel for abrasive particles to penetrate the material – for Al6061/Al_2O_3 (Hosseini et al., 2010). The microstructure resulting from a 4-hour MM process shows layered and folded grain shapes that are effortlessly removable from the worn surface. It is established that grains that are harder and thinner are more prone to fragility.

Figure 6. Weight loss (a), wear rate (b) and the coefficient of friction (c) of samples tested at different sliding distances.

The coefficient of friction results also indicates that particles or debris broken from the sample (because of the porous structure) during wear tests were easily removed from the tribological system. If the broken particles remained in the tribological system, the friction coefficient would be much higher. However, the friction coefficient is also an indication of the shear force that occurs on the sample/disc contact surface. The shear force generated by friction is also associated with the hardness of the material and with wear particles that cannot be removed from the tribological system. The hardness distribution in the surface layers also affects the wear. It has also been reported that the surface hardness should be lower than the deeper regions to avoid catastrophic results (Popov, 2019; Kragelski, 1965). Figure 6 shows that the surface layers have higher hardness than the inner regions, with a relatively greater difference observed on the sample MM'ed for 4 hours. This difference in hardness may be responsible for the higher weight loss observed in these samples. SEM images of nanocomposites MM'ed for varied durations are shown in Figure 7, illustrating example defects over the worn surface under a 30N load and after a 2000 m sliding distance.

Figure 7. SEM images of the worn surfaces of samples; a) A356 alloy, b) A356/nano Al_2O_3 samples MM'ed for 1h, c) A356/nano Al_2O_3 samples MM'ed for 2h, d) A356/nano Al_2O_3 samples MM'ed for 4h (SD: sliding direction, Spa: spalling, Del: delamination).

The first thing that stands out when the SEM images of the worn surface given in Figure 7 are examined is that the sliding lines (sliding directions) that occurred on the surface of the aluminium nanocomposites are evident. In addition, the plastic deformation that occurred on the surface of the composites due to friction and heat effect during the test can also be seen clearly. It is also observed that micro cracks formed on the surface because of plastic deformation on the composite-disc contact surfaces joined together to form local spallings later in the tests. In addition to plastic deformation, micropores also cause material to be removed from the surface of composites. Crater-shaped breakages/spallings can also be observed on the sample surfaces. However, in some previous studies, it was reported that the particles accumulated between the sample and the disc formed a lubricating oxide layer by sticking back to the sample and filling into the pores depending on the sliding distance (Sağlam et al., 2011). In addition, it was observed that there were narrow and wide channels parallel to the sliding direction on the composite sample surfaces. Plastic yield, which occurs together with narrow or wide channels, is also known to be an abrasive wear characteristic Kang and Chan, 2004). Accordingly, it was observed that abrasive and adhesive wear mechanisms occurred on composite sample surfaces in general. Wears caused by delamination can also be observed on the worn sample surfaces. Delamination wear is known as the removal of material in thin layers because of another surface on the sample surface (Jamaati et al., 2014). It was also reported in some previous studies that delamination breaking or peeling from the worn surfaces of Al-matrix micro or nano-particle reinforced composites were observed due to plastic deformation in addition to narrow and wide channels (Jamaati et al., 2014; Manivannan et al., 2017).

Conclusions

This study evaluates the effects of MM time on mechanical properties and the wear behavior of A356 aluminium matrix nanocomposites reinforced with 1%wt. Al_2O_3. The originality of the study is considering mechanical and wear properties by realizing the microstructural state provided by varied MM times. The wear performance of nanocomposites was investigated not only by hardness but also by microstructural outcomes. The general findings obtained from the study are outlined below.

(1) The average particle size underwent an increase after 2 hours of MM, which was attributed to the mechanisms of cold welding and bonding of powders. After 4 hours of MM, the particle size decreased by excessive deformation and work hardening of the powders.

(2) An increase in milling time led to a rise in porosity within the microstructure, caused by the formation of harder and more complex shaped grains, which in turn resulted in a decrease in the density of the nanocomposites.

(3) Despite the constant volume fraction of nanoparticle reinforcement, variations in MM time result in differing microstructures. One hour of MM time produces maintained grains with smaller size, while particles are bonded and grown in size with 2 hours of MM. 4 hours of MM, on the other hand, decreases the grain size by excessive deformation and fracture of the particles.
(4) The hardness of the nanocomposites improved with increasing MM time, resulting from the deformation hardening mechanism. The sample that underwent 4 hours of MM exhibited the highest hardness level among others and was the highest MM time in this study.
(5) Samples MM'ed for 1 hour exhibited the lowest weight loss and wear rate due to their higher density and moderate microstructure, while samples MM'ed for 2 and 4 hours showed higher weight loss values due to lower densities resulting in more particle detachment, and samples MM'ed for 4 hours exhibited the lowest friction coefficient values due to the presence of nano alumina particles acting as solid lubricants.

Conflict of interest

We declare that all authors have no conflict of interest.

References

Akbari, M., and Asadi, P. (2021), "Simulation and experimental investigation of multi-walled carbon nanotubes/aluminum composite fabrication using friction stir processing", Proceedings of the Institution of Mechanical Engineers, Part E: Journal of Process Mechanical Engineering, Vol. 235 No. 6, pp. 2165-2179.

Akbari, M., and Asadi, P. (2022), "Effects of different cooling conditions on friction stir processing of A356 alloy: Numerical modeling and experiment", Proceedings of the Institution of Mechanical Engineers, Part C: Journal of Mechanical Engineering Science, Vol. 236 No. 8, pp. 4133-4146.

Akbari, M., Asadi, P., and Asiabaraki, H. R. (2022), "Investigation of wear and microstructural properties of A356/TiC composites fabricated by FSP", Surface Review and Letters (SRL), Vol. 29 No. 10, pp. 1-10.

Akbari, M., Khalkhali, A., Keshavarz, S. M. E., and Sarikhani, E. (2018), "The effect of in-process cooling conditions on temperature, force, wear resistance, microstructural, and mechanical properties of friction stir processed A356", Proceedings of the Institution of Mechanical Engineers, Part L: Journal of Materials: Design and Applications, Vol. 232 No. 5, pp. 429-437.

Akhlaghi, F., Khakbiz, M. and Rezaii Bazazz, A. (2017), "Evolution of the size distribution of Al–B4C nano-composite powders during mechanical milling: a comparison of experimental results with artificial neural networks and multiple linear regression models", Neural Computing and Applications, Vol. 31 No. S2, pp. 1145–1154.

Archard, J.F. (1953), "Contact and Rubbing of Flat Surfaces", Journal of Applied Physics, Vol. 24 No. 8, pp. 981–988.

Bobić, B., Vencl, A., Ružić, J., Bobić, I., and Damnjanović, Z. (2019), "Microstructural and basic mechanical characteristics of ZA27 alloy-based nanocomposites synthesized by mechanical milling and compocasting", Journal of Composite Materials, Vol. 53 No. 15, pp. 2033-2046.

Çelebi, M., Çanakçi, A., Özkaya, S., and Karabacak, A. H. (2018), "The effect of milling time on the mechanical properties of ZA27/Al 2 O 3 nanocomposites", Universal Journal of Materials Science, Vol. 6 No. 5, pp. 163-169.

Edalati, K., Ashida, M., Horita, Z., Matsui, T. and Kato, H. (2014), “Wear resistance and tribological features of pure aluminum and Al–Al2O3 composites consolidated by high-pressure torsion”, Wear, Vol. 310 No. 1-2, pp. 83–89.

Erek, H.B., Özyürek, D. and Asan, A. (2017), “Corrosion Behaviour and Electrical Conductivity of Reinforced TiAl3and B4C Hybrid Aluminium Composites”, Acta Physica Polonica A, Vol. 131 No. 1, pp. 156–158.

Ezatpour, H.R., Torabi Parizi, M., Sajjadi, S.A., Ebrahimi, G.R. and Chaichi, A. (2016), “Microstructure, mechanical analysis and optimal selection of 7075 aluminum alloy based composite reinforced with alumina nanoparticles”, Materials Chemistry and Physics, Vol. 178, pp. 119–127.

Fogagnolo, J.B., Ruiz-Navas, E.M., Robert, M.H. and Torralba, J.M. (2003), “The effects of mechanical alloying on the compressibility of aluminium matrix composite powder”, Materials Science and Engineering: A, Vol. 355 No. 1-2, pp. 50–55.

Gibson, P. R., Clegg, A. J., and Das, A. A. (1984), “Wear of cast Al-Si alloys containing graphite”, Wear, Vol. 95 No. 2, pp. 193-198.

Güler, O., Çelebı, M., Dalmış, R., Çanakçi, A., and Çuvalci, H. (2020), “Novel ZA27/B 4 C/graphite hybrid nanocomposite-bearing materials with enhanced wear and corrosion resistance”, Metallurgical and Materials Transactions A, Vol. 51, pp. 4632-4646.

Hosseini, N., Karimzadeh, F., Abbasi, M. H., and Enayati, M. H. (2010), “Tribological properties of Al6061–Al2O3 nanocomposite prepared by milling and hot pressing”, Materials & Design, Vol. 31 No. 10, pp. 4777-4785.

Hosseini, N., Karimzadeh, F., Abbasi, M.H. and Enayati, M.H. (2012), “A comparative study on the wear properties of coarse-grained Al6061 alloy and nanostructured Al6061–Al2O3 composites”, Tribology International, Vol. 54, pp. 58–67.

Igor Viktorovich Kragel'skii. (1965), Friction and Wear, Buttersworths, London, pp. 2–15.

Jamaati, R., Naseri, M. and Toroghinejad, M.R. (2014), “Wear behavior of nanostructured Al/Al2O3 composite fabricated via accumulative roll bonding (ARB) process”, Materials & Design, Vol. 59, pp. 540–549.

Kang, Y.-C. and Chan, S.L.-I. (2004), “Tensile properties of nanometric Al2O3 particulate-reinforced aluminum matrix composites”, Materials Chemistry and Physics, Vol. 85 No. 2-3, pp. 438–443.

Manivannan, I., Ranganathan, S., Gopalakannan, S., Suresh, S., Nagakarthigan, K. and Jubendradass, R. (2017), “Tribological and surface behavior of silicon carbide reinforced aluminum matrix nanocomposite”, Surfaces and Interfaces, Vol. 8, pp. 127–136.

Mazahery, A. and Shabani, M.O. (2012), “Characterization of cast A356 alloy reinforced with nano SiC composites”, Transactions of Nonferrous Metals Society of China, Vol. 22 No. 2, pp. 275–280.

Moazami-Goudarzi, M. and Akhlaghi, F. (2016), “Wear behavior of Al 5252 alloy reinforced with micrometric and nanometric SiC particles”, Tribology International, Vol. 102, pp. 28–37.

Omidi, M., Khodabandeh, A., Nategh, S., and Khakbiz, M. (2017), “Wear mechanisms maps of CNT reinforced Al6061 nanocomposites treated by cryomilling and mechanical milling”, Tribology International, Vol. 110, pp. 151-160.

Ozyurek, D. and Ciftci, I. (2011), “An investigation into the wear behaviour of TiB2 particle reinforced aluminium composites produced by mechanical alloying”, Science and Engineering of Composite Materials, Vol. 18 No. 1-2, pp. 5–12.

Özyürek, D. and Tekeli, S. (2010), “An Investigation on Wear Resistance of SiCp-Reinforced Aluminium Composites Produced by Mechanical Alloying Method”, Science and Engineering of Composite Materials, Vol. 17 No. 1.

Özyürek, D., Yıldırım, M. and Çiftçi, İ. (2012), “The tribological properties of A356-SiCp metal-matrix composites fabricated by thixomoulding technique”, Science and Engineering of Composite Materials, Vol. 19 No. 4, pp. 351–356.

Popov, V. (2019), “Generalized archard law of wear based on rabinowicz criterion of wear particle formation”, Facta Universitatis, Series: Mechanical Engineering, Vol. 17 No. 1, p. 39.

Rahimian, M., Parvin, N. and Ehsani, N. (2010), “Investigation of particle size and amount of alumina on microstructure and mechanical properties of Al matrix composite made by powder metallurgy”, Materials Science and Engineering: A, Vol. 527 No. 4-5, pp. 1031–1038.

Safari, J., Akbari, G.H. and Delshad Chermahini, M. (2013), “The effect of reinforcement content and milling time on microstructure and mechanical properties of Al–10Mg/xAl2O3 nanocomposites”, Materials Science and Engineering: A, Vol. 569, pp. 86–91.

Sağlam, I., Özyürek, D. and Çetinkaya, K. (2011), “Effect of ageing treatment on wear properties and electrical conductivity of Cu-Cr-Zr alloy”, Bulletin of Materials Science, Vol. 34 No. 7, pp. 1465–1470.

Shivakumar, N., Vasu, V., and Narasaiah, N. (2015), “Synthesis and characterization of nano-sized Al2O3 particle reinforced ZA-27 metal matrix composites”, Procedia Materials Science, Vol. 10, pp. 159-167.

Simsek, D., Simsek, I. and Ozyurek, D. (2020), “Relationship between Al2O3 Content and Wear Behavior of Al+2% Graphite Matrix Composites”, Science and Engineering of Composite Materials, Vol. 27 No. 1, pp. 177–185.

Sunar, T., and Özyürek, D. (2022), “Effect of Al2O3 nanoparticles as reinforcement on the wear properties of A356/Al2O3 nanocomposites produced by powder metallurgy”, Journal of Tribology, Vol. 144 No. 8, pp. 081701.

Suryanarayana, C. (2001), “Mechanical alloying and milling”, Progress in Materials Science, Vol. 46 No. 1-2, pp. 1–184.

Tiku, V., Navin, K. and Kurchania, R. (2020), “Study of Structural and Mechanical Properties of Al/Nano-Al2O3 Metal Matrix Nanocomposite Fabricated by Powder Metallurgy Method”, Transactions of the Indian Institute of Metals, Vol. 73 No. 4, pp. 1007–1013.

Vencl, A., Bobić, I., Stanković, M., Hvizdoš, P., Bobić, B., Stojanović, B., and Franek, F. (2020), “Influence of secondary phases in A356 MMCs on their mechanical properties at macro-and nanoscale”, Journal of the Brazilian Society of Mechanical Sciences and Engineering, Vol. 42, pp. 1-12.

Vencl, A., Stojanović, B., Gojković, R., Klančnik, S., Czifra, Á., Jakimovska, K., and Harničárová, M. (2022), “Enhancing of ZA-27 alloy wear characteristics by addition of small amount of SiC nanoparticles and its optimisation applying Taguchi method”, Tribology and Materials, Vol. 1 No. 3, pp. 96-105.

Vencl, A., Vučetić, F., Bobić, B., Pitel, J., and Bobić, I. (2019), “Tribological characterisation in dry sliding conditions of compocasted hybrid A356/SiC p/Gr p composites with graphite macroparticles”, The International Journal of Advanced Manufacturing Technology, Vol. 100, pp. 2135-2146.

Yang, J. B., Lin, C. B., Wang, T. C., and Chu, H. Y. (2004), “The tribological characteristics of A356. 2Al alloy/Gr (p) composites”, Wear, Vol. 257 No. 9-10, pp. 941-952.

Yildirim, M., Özyürek, D. and Gürü, M. (2020), “Effect of Milling Time on Dry Sliding Wear Behaviors of Carbon Nanotubes Reinforced Al Matrix Composites”, Journal of Nanoscience and Nanotechnology, Vol. 20 No. 4, pp. 2633–2638.